

Implementation of Low Power Consumption of Neuromorphic Devices

Takahiro Toizumi^{1,a}, Yoshiki Sasaki^{2,b} and Katsutoshi Saeki^{1,2,c}

¹ Graduate school, Nihon University

7-24-1, Narashinodai, funabashi, Chiba 274-8501, Japan

² Collage of science and technology, Nihon University

7-24-1, Narashinodai, funabashi, Chiba 274-8501, Japan

E-mail: ^acstkt16007@g.nihon-u.ac.jp, ^bsasaki.yoshiki@nihon-u.ac.jp, ^csaeki.katsutoshi@nihon-u.ac.jp

Abstract:

For a large scale artificial neural network, it is desirable that a neuromorphic device constructing presents low power consumption.

Previously, we proposed a cell body model with a reduced mounting area, with a power consumption was 4.2 [mW]. In this model, the gate voltage of the N-channel type MOSFET (NMOS) as a negative resistance device was more than the voltage that the IC can withstand.

In this paper, we reduce the gate voltage of this NMOS, resulting in a neuromorphic device with a gate voltage lower than 2.2 [V]. Furthermore, it is clearly shown that its power consumption is approximately 16.6% lower than the previous proposed model.

1. Introduction

Brain neural network presents excellent information processing mechanism, leading many investigators to model biological neurons and their networks. Recent neural networks studies have been undertaken with the purpose of applying engineering to the brain function [ref. 1, 2, 3, 4]. As a method for modeling the information processing function of the brain, the artificial neural network (ANN) has been suggested. Therefore, it is necessary to construct ANN using neuromorphic devices, which is the features of the neuron. When a large-scale ANN is constructed, it is desired that its neuromorphic device has a small area and low power consumption.

Analog LSI neuron model for similar biological excitable membrane operation has been proposed by Kano et al [ref. 5]. The model simulates excitations observed in neurons of the living body using voltage-controlled negative resistance characteristics. The action potential generation mechanism is similar to the neurons of the living body. As a result, this model presents vertical length of 60 [μm]; horizontal length of 180 [μm]; and power consumption of approximately 240 [μW] without input and 8.3 [mW] at firing time.

Previously, we proposed a cell body model [ref. 6] with a reduced the area, using the parasitic capacitance and the N-channel MOSFETs (NMOS). The power consumption of this model is approximately 4.2 [mW]. However, the gate voltage of the NMOS, which is a negative resistance device, became greater than the breakdown voltage. In this paper, we study the implementation of a neuromorphic device with low power consumption by focusing on the gate voltage of NMOS as a negative resistance device.

2. Neuromorphic device

Figure 1 shows a circuit diagram of the proposed neuromorphic device. Circuit parameters are $M_N = 60$, $M_D = 0.6$, $M_C = 1$, $M_R = 0.67$, $M_T = 20$, and power-supply voltage $V_A = V_D = 1.8[\text{V}]$. Furthermore, C_{g1} , C_{g2} and C_M are parasitic capacitances.

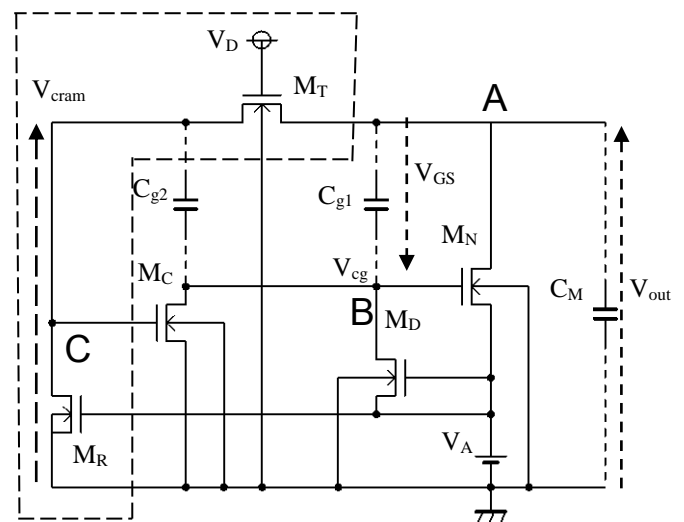


Figure 1 Proposed neuromorphic device

The principle of Figure 1 is shown as follows. In the initial condition, if V_{out} , V_{cg} and V_{cram} is 0 [V], drain-source voltage of M_T and M_R are both 0 [V]. Hence, there is no drain-source current on M_N and M_C . the gate-source voltage of M_C and M_N is also 0 [V], resulting in a null drain-source current on M_C and M_T . C_{g1} and C_{g2} are supplied with the charge of V_A through M_D . Since C_{g1} charge does not flow through M_T , it flows into C_M , resulting in small V_{out} . Furthermore, when there is electric potential difference of drain-source voltage of M_T and M_R , current flows from the former's drain to the latter's source. When V_A increases, C_{g1} and C_{g2} are charged, and there is an increase on M_N gate-source voltage (V_{GS}). V_{GS} is greater than threshold voltage, results in large drain-source current of M_N . Because W/L of M_N is greater than W/L of M_T and M_R , the surplus current does not flow in M_T nor M_R . As a result, it flows into C_M , and V_{out} rises up. In addition, V_{cram} also rises up and gate-source voltage of M_C becomes more the threshold voltage. Therefore, drain-source current of M_C begins to flow. M_C pulls out the charge of C_{g1} and C_{g2} , and then V_{GS} goes down. As a result, when V_{GS} is near to 0 [V], current does not flow in M_N . When the charge accumulated in C_M dissipates through M_T and M_R , V_{out} goes down, and then V_{cram} also goes down. Hence, the current does not flow

in M_C . The proposed neuromorphic device repeats the oscillation by again accumulating the charges in C_{g1} and C_{g2} through M_D from V_A .

Figure 2 shows the output waveform while Figure 1 shows the gate potential of M_N . It can be seen that the gate potential of the NMOS as a negative resistance device is suppressed to less than or equal to the breakdown voltage, 2.2 [V].

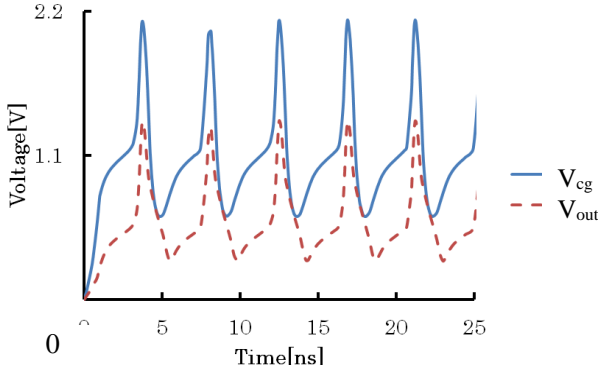


Figure 2 Voltage characteristics of proposed neuromorphic device

On the conventional model, V_{cg} is the gate voltage of NMOS as a negative resistance device. It can be expressed as

$$V_{cg} = V_{out} + V_{GS} \quad (1)$$

In this equation, V_{out} is voltage across C_M . V_{GS} is the gate-source terminal voltage of M_N . From the above equation, V_{cg} is reduced by reducing V_{out} or V_{GS} . In order to reduce the V_{cg} , the following improvements are required to the conventional model.

- (i) Insertion of M_T
- (ii) Connection of the parasitic capacitance between V_{cg} and drain-source terminal of M_T
- (iii) Increase of the aspect ratio of M_N

Figure 3 shows a circuit diagram of a clamp circuit including a M_T . In this figure, circuit parameters are $M_T = 20$, $M_R = 0.67$, $V_A = V_D = 1.8$ [V]. In Figure 1, the part surrounded by a dotted line corresponds to Figure 3. Figure 4 shows the characteristics of the latter. When the peak-to-peak voltage of $V_{out} = \pm 1.8$ [V] and frequency is 333 [MHz], it shows V_{out} and V_{cram} characteristics. It can be seen that V_{cram} is clamped by approximately ± 1 [V]. Thus, by inserting M_T , point C in Figure 1 has a potential lower than V_{out} .

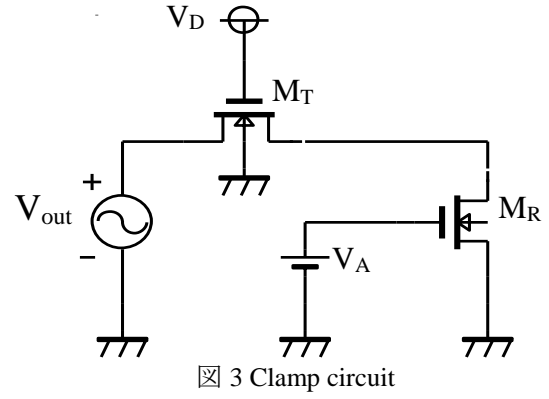


Figure 3 Clamp circuit

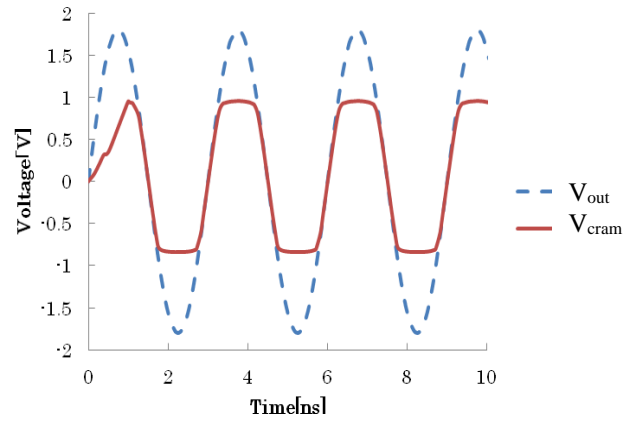


Figure 4 Voltage characteristics of clamp circuit

In the conventional model, the gate of M_C was connected to V_{out} . Therefore, the parasitic capacitance was connected only between V_{out} and V_{cg} . Hence, V_{cg} was influenced by only V_{out} and V_{GS} according to the parasitic capacitance between A and B. However, in the proposed neuromorphic device, the gate of M_C is connected to C by inserting the M_T . Further, in the conventional model, the parasitic capacitance between A and B was composed by the parasitic capacitance between drain and gate of M_C and between gate and source of M_N . Therefore, by connecting the gate of the M_C in C, appears a parasitic capacitance between B and C. The potential of V_{cg} , which was only influenced by V_{out} in the conventional model, is reduced by the influence of V_{cram} .

Then, the aspect ratio of the M_N was increased. Consequently, when V_{out} rises, the drain-source current of M_N increases. Since the amount of current flowing into the C_M increases, V_{out} increases. When V_{out} rises faster than a conventional model, V_{cram} rises fast, too. Therefore, the drain-source current of M_C flows faster than the conventional model. It is possible to reduce V_{cg} by withdrawing charges from C_{g1} and C_{g2} before the potential of V_{cg} rises high. Figure 5 shows changes in V_{cg} of the proposed neuromorphic device when changing the aspect of M_N . It is seen that, by increasing the aspect ratio of the M_N , V_{cg} reduces.

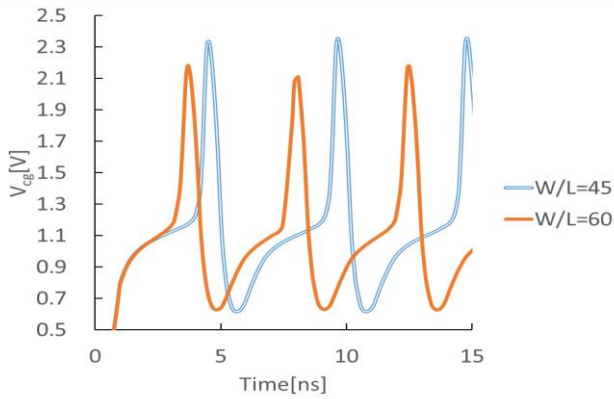


Figure 5 V_{cg} characteristics regarding the aspect ratio in M_N

3. Refractory period

Figure 6 shows the refractory period characteristics of the proposed neuromorphic device. Δt represents a time interval to input I_{in} as reproduction signal of another neuron model from outside. V_{out1} and V_{out2} shows the peak value of V_{out} after the first and second time of I_{in} , respectively. Hence, neuromorphic devices are the separately excited cell body model. Figure 6 represents the change in the firing condition for the input period. It is shown that the neuromorphic device does not fire on the second time of I_{in} when the input period Δt is short. Therefore, it can be seen that neuromorphic device has a refractory period characteristics.

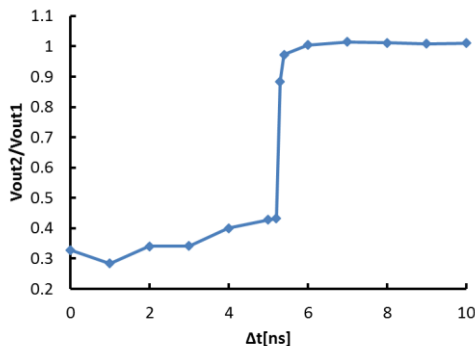


Figure 6 Refractory period characteristics

Figure 7 shows the relative refractory period characteristics of the proposed neuromorphic device. The figure represents the change in the firing state for second input of neuromorphic device, when Δt is 4 [ns] and the peak value of input has been increased. In this figure, it is shown that the neuromorphic device can oscillate when I_{in} increase, while the refractory period. Therefore, it can be seen that the proposed neuromorphic device has a relative refractory period characteristics.

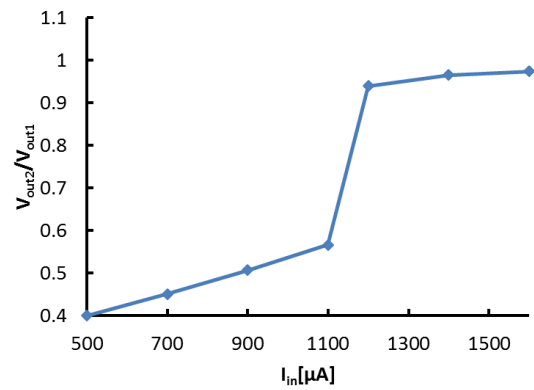


Figure 7 Relative refractory period characteristics

4. Chaotic response

Figure 8 shows the input-output frequency characteristics of the proposed neuromorphic device. f_{in} represents the frequency of I_{in} , while f_{out} indicates the oscillation frequency of V_{out} . Drawing effect 1:1, 1:2 and 1:3 can be observed. Figure 9 shows the attractor of the proposed neuromorphic device when input period is 2.75 [ns] ($f_{in} = 0.36$ [GHz]). From the above reason, it suggests that chaotic response is obtained from the proposed neuromorphic device.

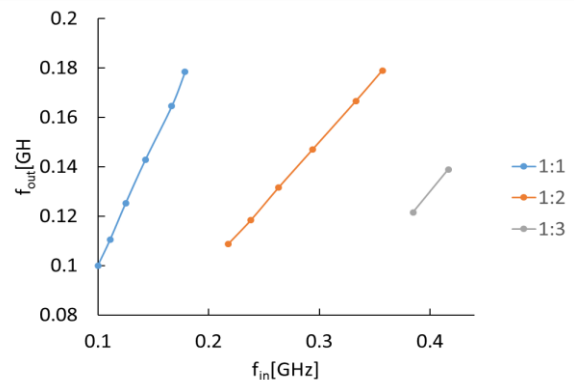


Figure 8 Input-output frequency characteristic

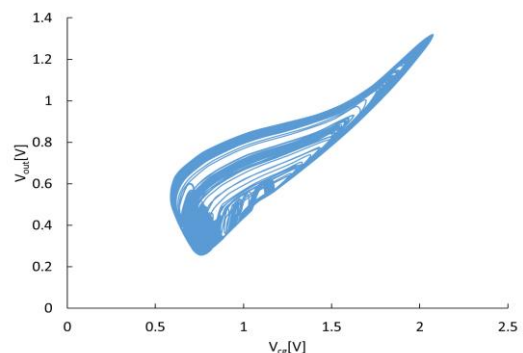


Figure 9 Attractor

5. Layout

Figure 10 shows layout diagram of the neuromorphic device. From Figure 3, the vertical length is approximately 9.6 [μm], the horizontal length is approximately 14.9 [μm]. Therefore, the proposed device mounting area is

approximately 142.6 [μm^2], which is almost same as that of the conventional model.

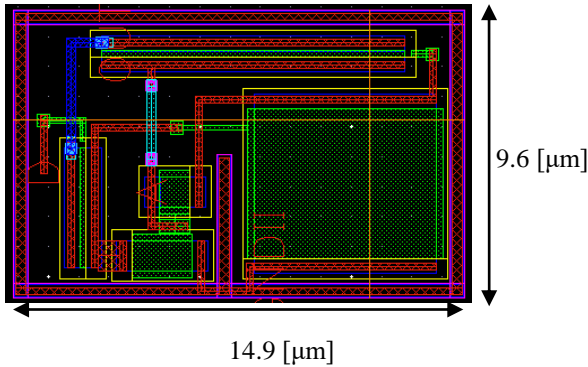


Figure 10 Layout of the proposed neuromorphic device

6. Power consumption

Figure 11 shows the current characteristics of I_A and I_D , which is flowing through V_A and V_D , respectively. The power consumption of the proposed neuromorphic device is approximately 696.8 [μW]. On the other hand, the power consumption of a conventional device is about 4.2 [mW]. Table 1 compares power consumption of both devices. It shows reduction of up to 16.6% when compared with the latter.

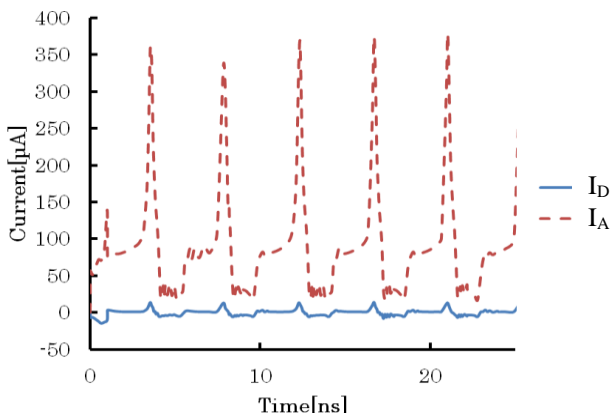


Figure 11 Current characteristics of power supply

Table 1 Power consumption comparison

	Power consumption
Conventional model	4.2 [mW]
Proposed neuromorphic device	696.8 [μW]

7. Conclusion

In this paper, we examined the implementation of low power consumption of a neuromorphic device by focusing on the gate voltage of NMOS as a negative resistance device. As a result, we constructed a neuromorphic device with a gate voltage of less than 2.2 [V]. Furthermore, it was clearly shown that its power consumption was reduced to approximately 16.6%, when compared with the conventional model.

In future work, we will construct a large-scale neural network using a neuromorphic device.

Acknowledgements

This work has been supported in part by JSPS KAKENHI Grant Number #25420344. Furthermore, the VLSI chip in this study has been fabricated in the chip fabrication program of VLSI Design and Education Center (VDEC), the University of Tokyo in collaboration with Rohm Corporation and Toppan Printing Corporation.

References

- [1] Makoto Itou, Jousuke Kuroiwa, Shougo Miyake, (1999), A Neural Network Model of Memory System Using Hippocampus, The transactions of the Institute of Electronic, Information and Communication Engineers J82-D-II, pp. 276-286
- [2] Motoharu Yoshida, Hatsuo Hayashi, Satoru Ishizuka, (2002), Sequential Memory Recall Model of The Hippocampal Taking Advantage of Propagation of Neuronal Activity in CA3, IEICE, 101, pp. 1-7
- [3] Keisuke Wada, Katsutoshi Saeki, Yoshifumi Sekine, (2009), A Study on Dentate Gyrus-CA3 Electronic Circuits Model with Spatial Summation, ECT, pp. 47-52
- [4] Yoshifumi Sekine, Katsutoshi Saeki, (2008), CMOS Implementation of Pulse-type Hardware Neuron Model and Its Application, The Brain and neural network 15, pp. 27-38
- [5] Shinichiro Kanoh, Makoto Imai, Nozomu Hoshimiya, (), Analog LSI Neuron Model Inspired by Biological Excitable Membrane, Institute of Electronics, Information and Communication Engineers D-II Vol. J86-D-II No. 8, pp. 1254-1261
- [6] Atsushi Okuyama, Katsutoshi Saeki, Yoshifumi Sekine, (2014), A Study on Reduced Area of a Cell Body Model for an Artificial Neural Network, Nihon University Academic Lecture Papers, M-17, pp. 1105-1106